Dopamine receptor D1 agonist inhibits glioblastoma via calpain-mediated ER stress and mitochondrial dysfunction

KANG YANG[1], RUIXUE XU[2] and WEIDONG LE[3,4]

[1]Department of Neurosurgery, The Second Hospital of Dalian Medical University; [2]Department of Neurosurgery; [3]Liaoning Provincial Center for Clinical Research on Neurological Diseases; [4]Liaoning Provincial Key Laboratory for Research on Pathogenic Mechanisms of Neurological Diseases, The First Hospital of Dalian Medical University, Dalian, Liaoning 116000, P.R. China

Received October 12, 2020; Accepted February 18, 2021

DOI: 10.3892/or.2021.8025

Abstract. Recent studies have reported the important roles of dopamine receptors in the early development and progression of glioblastoma (GBM). The present research aimed to explore the antineoplastic effect and intrinsic pathways of action of dopamine receptor D1 agonist SKF83959 on GBM cells. Flow cytometric analysis revealed a significant level of apoptotic cell death under SKF83959 treatment. SKF83959 administration increased intracellular calcium levels and oxidative stress through the phospholipase C/inositol trisphosphate pathway. The downstream calpains were activated and dysregulated by the increased calcium levels. The mitochondrial membrane potential-dependent staining assay revealed decreased mitochondrial transmembrane potential in GBM cells under SKF83959 treatment. The mitochondrial/cytosolic fraction and western blotting further demonstrated mitochondrial dysfunction and endoplasmic reticulum stress, followed by apoptosis. The calpain inhibitor, calpastatin, significantly reversed the increase in mitochondrial injury and endoplasmic reticulum stress and eventually ameliorated GBM cell apoptosis during SKF83959 treatment. Finally, the *in vivo* inhibitory efficacy of SKF83959 was verified in GBM xenograft models. In addition, immunohistochemistry and western blotting both revealed increased expression of calpains in xenograft GBM tissues. These results suggested a potential therapeutic target for human GBM treatment regarding calpain expression and activity regulation.

Correspondence to: Professor Weidong Le, Liaoning Provincial Center for Clinical Research on Neurological Diseases, The First Hospital of Dalian Medical University, 193 Lianhe Street, Dalian, Liaoning 116000, P.R. China
E-mail: wdle_sibs@126.com

Key words: glioblastoma, apoptosis, tumorigenesis, calpain, endoplasmic reticulum stress, mitochondrial dysfunction

Introduction

Glioblastoma (GBM) is the most deadly yet common form of primary central nervous system tumours, and accounts for approximately 53.7% of all gliomas (1). Only 4.75% of patients diagnosed with GBM survive for 5 years (2,3). The inevitable therapeutic failure and poor prognosis partially result from the highly invasive feature of GBM by infiltrating surrounding structures through preferential anatomical pathways, which leads to incomplete surgical resection and consequent tumour recurrence (4-6). Although a significant amount of work has been conducted to find the intracellular factors facilitating the infiltrative nature of GBM cells, the underlying molecular mechanisms remain unclear.

Calcium (Ca^{2+}) is reported to be involved in the tumorigenesis, survival, invasion and apoptosis of cancer cells (7,8). Calpains are a group of Ca^{2+}-activated cysteine proteinases that consist of a regulatory and a catalytic subunit (9). Various studies have documented that tumour invasion can be enhanced by calpains (10-13). Calpains are also abundantly expressed in GBM cells and are implicated in cell invasion and migration of GBM (14-17). The *in vivo* evidence has revealed that inhibition of calpains can suppress the angiogenesis of pulmonary microvascular endothelial cells via vascular endothelial growth factor (18). Jang *et al* demonstrated by *in vitro* Transwell assays that reduced calpain 2 expression decreased the invasive capacity of GBM cells (14). Calpains have also been revealed to be involved in regulating cancer cell apoptosis and executing necrosis (19).

Apoptosis is a well-known type of programmed cell death that plays a crucial role in cancer maintenance and development as well as inhibition during chemotherapy (20). In response to chemotherapeutic drugs, overexpression of proapoptotic proteins could provide GBM cells a survival advantage (21). Wick *et al* and Stegh *et al* have also demonstrated that apoptosis resistance through overexpression of Bcl-2 (an antiapoptotic protein) in GBM cells increased tumour migration and invasion (22,23). The intrinsic pathways leading to apoptosis include mitochondrial dysfunction, oxidative stress, endoplasmic reticulum (ER) stress and production of reactive oxygen species (ROS) (24-29). It has recently been documented that calpains trigger an apoptotic cascade via

several pathological factors, such as oxidative stress, induction of mitochondrial injury and activation of ER stress (29-34). Guan *et al* have demonstrated that expression and activation of calpains facilitate mitochondrial fission, inducing cardiomyocyte apoptosis. Inhibition of calpains by calpastatin (an endogenous calpain inhibitor) enhanced mitophagy and mitochondrial fusion, and inhibited apoptosis and excessive mitochondrial fission (35). Cho *et al* have reported that inhibition of calpain activity alleviated DNA cleavage induced by oxidative stress, and apoptosis in pancreatic acinar cells (36).

In our previous study, it was reported that treatment with dopamine receptor D1 (DRD1) agonist, SKF83959, yielded a therapeutic effect against GBM both *in vitro* and *in vivo* (37). In the present study, the complex interplay between DRD1-agonist-induced GBM cell apoptosis and possible signalling pathways related to downstream molecules of Ca^{2+} accumulation were explored. The aim of the present study, was to investigate an alternative avenue for the design of future GBM therapies.

Materials and methods

Collection of human GBM samples and control brain tissues. A total of 4 female and 6 male patients (mean age, 56.3±7.7 years) diagnosed as GBM with both typical clinical symptoms (including headache, nausea, vomiting, motor or sensory disturbance, speech or swallowing difficulties or other manifestations of focal neurological deficits) and MRI scans (diagnosed by at least two radiologists) were hospitalized at the Department of Neurosurgery, the Second Hospital of Dalian Medical University (DMU; Dalian, China) between January 2016 and January 2018. The surgical resection and collection of GBM samples were approved by the Ethics Committee of the Second Hospital of Dalian Medical University (approval no. 2018052), following the ethical guidelines of the Declaration of Helsinki. Written consent was obtained from all patients. The resected GBM samples were diagnosed as the World Health Organization (WHO) grade IV by at least two pathologists. The control brain tissues (n=10) were obtained from negative margins of intracranial hematoma patients (4 females and 6 males; mean age: 59.4±6.8 years), who had no neuropathological evidence of brain tumours or history of brain trauma, encephalitis, meningitis or epilepsy.

Cell culture and measurement of cell viability. The human U87 GBM (GBM of unknown origin; cat. no. TCHu138) and mouse N2a neuroblastoma (cat. no. TCM29) cell lines were purchased from the Cell Bank of the Chinese Academy of Sciences (Shanghai, China), which has authenticated the cell lines by STR profiling. Cells were cultured in Dulbecco's modified Eagle's medium (C11995500BT; Gibco; Thermo Fisher Scientific, Inc.) containing 10% foetal bovine serum, with 5% CO_2 supplementation at 37˚C. Measurement of cell viability was conducted with CCK-8 assay (product code CK04; Dojindo Molecular Technologies, Inc.). The compounds applied were: SKF83959 hydrobromide (cat. no. 2074; Tocris Bioscience; 0-50 μM) was used at 37˚C for 0-72 h; BAPTA-AM (cat. no. S7534; Selleck Chemicals; 500 nM) was applied at 37˚C for 48 h; U73122 (cat. no. S8011; Selleck Chemicals; 1-2 μM) was used at 37˚C for 48 h, and calpastatin (cat. no. 2950; Tocris Bioscience; 25 nM-1 μM) was used at 37˚C for 48 h. After the addition of CCK-8 reagent (10 μl) to all wells where cells were plated, the reaction plates were incubated for 2 h at 37˚C. A microplate reader (Tecan Infinite F200/M200) was used to detect the absorbance at 450 nm.

Western blotting. Cells were collected and lysed in RIPA buffer (product no. P0013C; Beyotime Institute of Biotechnology). A BCA protein assay kit (cat. no. T9300A-3; Takara Biotechnology Co., Ltd.) was used to evaluate the protein concentration. Western blotting was conducted according to standard protocols. Cellular proteins (50 μg) were separated by gradient 4-15% SDS-PAGE gels (cat. no. 4561086; Bio-Rad Laboratories, Inc.). The transferred PVDF membranes (Immobilon; EMD Millipore) were incubated with primary antibodies at 4˚C overnight and secondary antibodies at room temperature (RT) for 1 h. The primary antibodies were purchased and used as followings: Anti-cleaved caspase-3 (product no. 9661; 1:1,000), anti-caspase-3 (product no. 9662; 1:1,000), anti-cleaved caspase-8 (product no. 9496; 1:1,000), anti-caspase-8 (product no. 4790; 1:1,000), anti-CHOP (product no. 2895T; 1:1,000), anti-BiP (product no. 3177T; 1:1,000), anti-GAPDH (product no. 2118; 1:1,000), and anti-cytochrome *c* (Cyt *c*) (product no. 4272s; 1:1,000) all from Cell Signaling Technology, Inc., anti-COX IV (product code ab14744; 1:1,000; Abcam), anti-Bcl-2 (product code ab692; 1:1,000; Abcam), anti-calpains (cat. no. sc-58326, 1:500; Santa Cruz Biotechnology, Inc.), and anti-β-actin (product no. A5441; 1:5,000; Sigma-Aldrich; Merck KGaA). The secondary antibodies were anti-rabbit/mouse IgG, HRP-linked antibody (product nos. 7076 and 7074; 1:2,000; Cell Signaling Technology, Inc.). ECL was used as the visualisation reagent (product no. P0018FM; Beyotime Institute of Biotechnology). A FluorChem Q system was used to quantify the target protein bands, which were then evaluated by Alpha View SA software (both from ProteinSimple).

Mitochondria and cytoplasm extraction. The mitochondrial and cytosolic proteins were extracted with Tissue Mitochondria Isolation Kit (product no. C3601; Beyotime Institute of Biotechnology). Cells ($2x10^6$) were washed with PBS and collected by centrifugation (600 x g for 5 min, 4˚C), and then resuspended with 1.5 ml mitochondrial extraction buffer and stored on ice for 10 min. The cellular suspension was homogenized with a Teflon-glass homogenizer with 10-15 up-and-down passes of the pestle. The homogenate was then centrifuged at 750 x g for 10 min (4˚C). The supernatants were centrifuged at 11,000 x g for 10 min (4˚C). The sediments were suspended to acquire mitochondria, while the resulting supernatants were centrifuged at 12,000 x g for 10 min (4˚C) to acquire the cytosolic proteins.

Immunohistochemistry. Formaldehyde-fixed (10%, at 4˚C, overnight), paraffin-embedded GBM tissue sections were boiled in sodium citrate buffer (pH 6.0) for 30 min using a microwave histoprocessor for antigen retrieval. Tissue sections were dehydrated and subjected to peroxidase blocking (3% hydrogen peroxide, at RT for 10 min). All brain tissues were cut into 4-μm sections. Then they were incubated with

primary antibody at RT for 1 h and then were incubated with 100 μl enhanced HRP-conjugated secondary antibody at RT for 20 min (product no. PV-9002; ZSGB-BIO; OriGene Technologies, Inc.). The primary antibody used was anti-calpain (cat. no. sc-58326; 1:500; Santa Cruz Biotechnology, Inc.). After washing, sections were covered with mounting medium and imaged with a fluorescence microscope.

Detection of intracellular Ca^{2+} levels. The Fluo-4 AM detection kit (product no. S1060; Beyotime Institute of Biotechnology) was used to evaluate the intracellular Ca^{2+} level in U87 cells. Cells ($5x10^4$) were firstly plated in 96-well culture plates for 24 h. After washing with PBS, cells were loaded with Fluo-4 AM reagent for 30 min at 37˚C in Hank's Balanced Salt Solution (HBSS; Invitrogen; Life Technologies; Thermo Fisher Scientific, Inc.) and incubated for another 30 min at room temperature. The cells were washed with HBSS followed by fluorescence recording at 37˚C with a Flouroskan Ascent (emission at 538 nm and excitation at 485 nm; Thermo Electronic Corporation; Thermo Fisher Scientific, Inc.) every 6 sec. Fluorescence microscopy was also used to visualize the fluorescent intensity of Fluo-4 AM probe in SKF83959-treated U87 cells.

ROS detection. Cells ($5x10^4$) were incubated in PBS with 10 μM DCFH-DA (product no. S0033; ROS Assay Kit; Beyotime Institute of Biotechnology) and 5.5 mM glucose supplement for 20 min at 37˚C. After incubation in common culture medium for another 10 min, the ROS levels in cells were detected using a microplate reader (Tecan Group, Ltd.).

Mitochondrial transmembrane potential Assay. The Mito-Tracker Red CMXRos kit (product no. C1035; Beyotime Institute of Biotechnology) was used to evaluate the mitochondrial transmembrane potential in U87 cells. Cells ($5x10^5$) were firstly treated with SKF83959 (35 μM) and/or BAPTA (500 nM) for 24 h. After washing with PBS, cells were stained with 50 nM Mito-Tracker Red CMXRos reagent for 30 min at 37˚C and nuclei were stained with Hoechst at RT for 5 min. Red fluorescence images were recorded under fluorescence microscopic observation and the fluorescence intensity was measured using ImageJ software 2.1 (National Institutes of Health).

Flow cytometric analysis. After treatment with SKF83959 (35 μM) at 37˚C for 72 h, U87 and N2a cells ($2x10^6$) were collected and the Annexin V and PI staining-based fluorescein isothiocyanate Annexin V Apoptosis Detection kit (BD Biosciences) was used to assess cell apoptosis, according to the manufacturer's instructions. The flow cytometry (BD FACSCanto II; BD Biosciences) and BD FACSDiva™ 7.0 software (BD Biosciences) were used for analysis for early + late apoptotic cells.

Cell cycle analysis. Pretreated cells ($2x10^6$) were collected and maintained in 70% ethanol at 4˚C for at least 24 h. After RNA degradation by RNase A (100 μg/ml; product no. GE101-01; TransGen Biotech Co., Ltd.) at 37˚C for 30 min, cells were then stained with PI (50 μg/ml; BD Pharmingen; BD Biosciences) on ice for 30 min and assessed by flow cytometry (BD FACSCanto II; BD Biosciences). The data was collected by BD FACSDiva™ 7.0 software (BD Biosciences) and analyzed by ModFit LT 4.0 software (BD Biosciences) according to the manufacturer's instructions.

Xenograft experiments. A total of 10 female BALB/c mice (weight, 18-20 g) were purchased from the Institute of Genome-Engineered Animal Models of Dalian Medical University and kept under specific pathogen-free conditions. The housing conditions were as follows: Temperature 22±2˚C, 12-h light/12-h dark cycle, relative humidity 60±15% and autonomous intake of water and food. U87 cells ($1x10^7$) mixed in PBS were subcutaneously injected into the flanks of 5-week-old immunocompromised athymic nude mice. The mice were intraperitoneally treated with SKF83959 (1 mg/kg/day) or the same amount of saline (n=5 in each group). The tumour volumes were measured every other day. The mice were sacrificed humanely by CO_2 asphyxiation with displacement of CO_2 (in 30%/min) at the same end point. The protocol was approved by the Animal Ethics Committee of Dalian Medical University (approval no. 2018112).

Statistical analysis. Statistical analysis was conducted with GraphPad Prism 6 (GraphPad Software, Inc.). Unpaired Student's t-tests were used to determine statistical differences between treatment and control groups. Comparisons among multiple groups were performed using one-way analysis of variance (ANOVA) followed by Tukey's (for multiple comparison between 4 or more groups) and Dunnett's (for comparison with one control group) post hoc tests. $P<0.05$ was considered to indicate a statistically significant difference.

Results

DRD1 agonist leads to apoptotic GBM cell death. A CCK-8 assay was used to evaluate the cytotoxicity of DRD1 agonist SKF83959 in human GBM cell line U87; one of the most common GBM cell models to date. SKF83959 revealed a significant inhibitory effect in a time-dependent (0-72 h) and concentration-dependent (0-50 μM) manner (Fig. 1A). The proportion of viable U87 cells was markedly decreased to 51.8% by SKF83959 at 35 μM for 48 h. Therefore, 35 μM was selected as the intervention concentration for the following experiments. To investigate whether apoptotic death was involved in the inhibitory effect, flow cytometric analysis was used to compare the apoptotic rate between U87 cells treated with DRD1 agonist and the non-GBM cell line N2a as a control. Quantification of apoptosis is the early + late apoptosis rate (n=3). SKF83959 treatment at 35 μM for 72 h induced 27.3% apoptotic cell death, while the apoptotic rate of N2a cells was only 9.5%, which validated the selectivity of SKF83959-induced apoptosis towards GBM cells (Fig. 1B). Western blotting revealed the protein levels of full and cleaved caspase-8 and caspase-3, typical apoptosis markers (36). To determine the apoptotic status regarding caspase-3 and caspase-8 activation, the ratio between cleaved and full caspase-3/8 (and rationalized to endogenous control) was analysed. The results revealed that the ratios were increased in U87 cells treated with SKF83959 in a time-dependent (0-48 h)

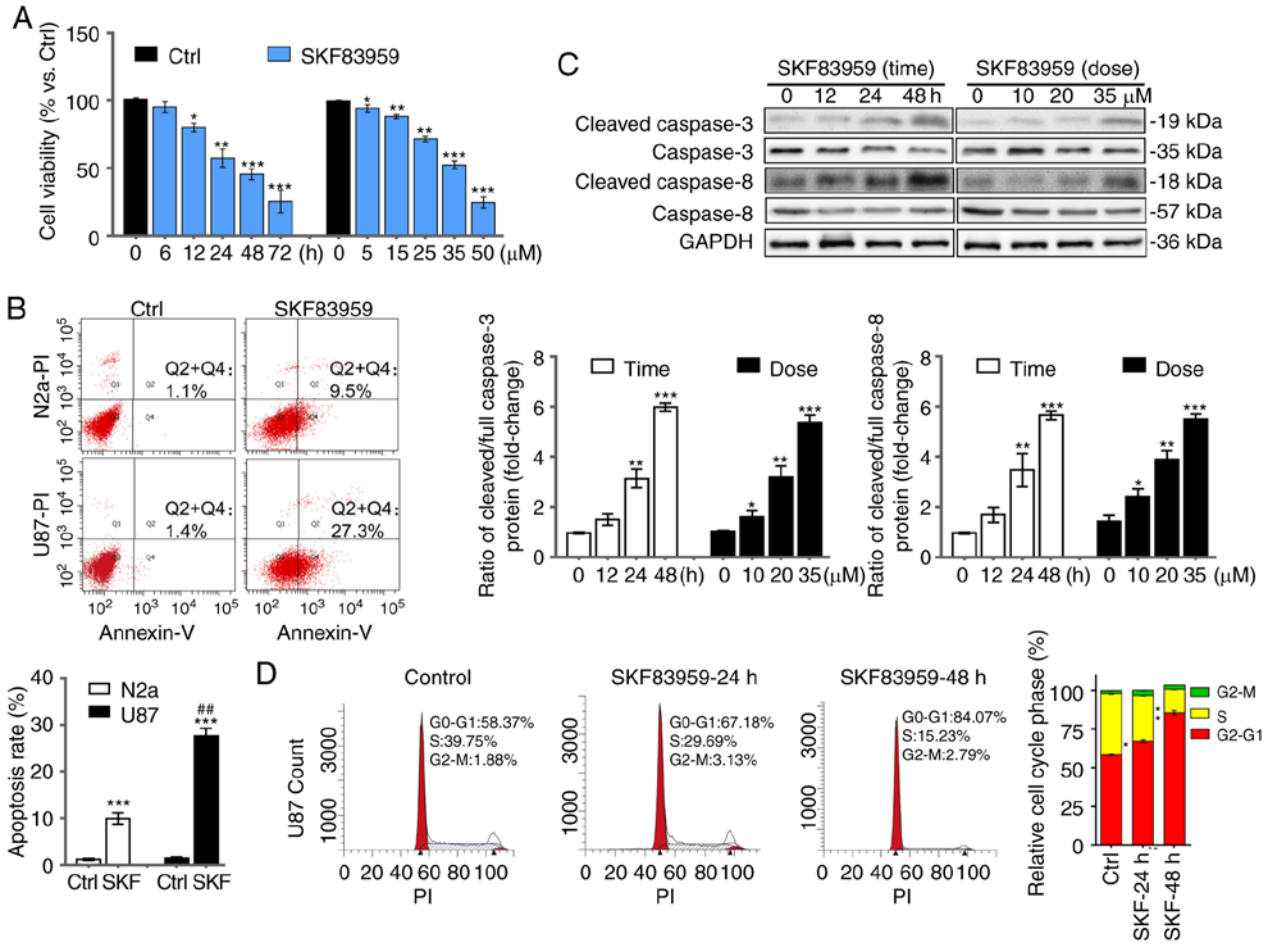

Figure 1. DRD1 agonist leads to apoptotic GBM cell death. (A) Viability of U87 cells treated with SKF83959 at 0-50 μM or for 0-72 h. (B) Apoptosis of U87 and N2a cells treated with SKF83959 (35 μM) were detected by flow cytometry after staining with Annexin V and PI. Quantification of apoptosis is the early + late apoptosis rate (n=3). (C) Expression levels of full and cleaved caspase-3 and caspase-8 in U87 cells treated with SKF83959 at 0-35 μM or for 0-48 h were determined by western blotting. The apoptotic status regarding caspase-3 and caspase-8 activation was analysed by calculating the ratio between the cleaved and full caspase-3/8 (and rationalized to endogenous control). (D) Cell cycle analysis of U87 cells treated with SKF83959 (35 μM) was performed by flow cytometry. Quantification of DNA contexts at different stages is presented on the right (n=3). *P<0.05, **P<0.01, and ***P<0.001 (vs. Ctrl); $^{\#\#}$P<0.01 (U87 vs. N2a cells with SKF83959). DRD1, dopamine receptor D1; GBM, glioblastoma; Ctrl, control; SKF, SKF83959.

and concentration-dependent (0-35 μM) manner (Fig. 1C). DNA content was further analysed in U87 cells treated with SKF83959 (35 μM) and a worsening G_0/G_1 arrest over time was detected (Fig. 1D), suggesting that cell cycle arrest was triggered by this agonist, which may have been followed by apoptosis.

DRD1 agonist increases PLC-dependent intracytosolic Ca^{2+} levels and induces oxidative stress. D1-like receptors are known to upregulate PLC, which is a major contributor to intracellular Ca^{2+} release (38-41). An increased level of intracytosolic Ca^{2+} after SKF83959 treatment (0, 10, 20, 35 μM) was observed as demonstrated by increased fluorescent intensity in treated Fluo-4 AM-loaded U87 cells (Fig. 2A). Then, the PLC inhibitor, U73122, was used to evaluate whether PLC signalling was involved. By measuring the intracytosolic Ca^{2+} after SKF83959 treatment (35 μM), a significant reversal of intracytosolic Ca^{2+} level in the presence of 2 μM U73122 was observed (Fig. 2B). GBM cell inhibition by SKF83959 was also ameliorated when co-treated with U73122, which suggested the involvement of PLC in the apoptotic signalling pathway (Fig. 2C).

Oxidative stress was then focused on, such as ROS generation, an important intrinsic pathway leading to apoptotic cell death, which can be induced by an increased intracytosolic Ca^{2+} level (24-29). ROS assays were used to detect ROS, and increased levels were revealed in U87 cells treated with SKF83959 in a time- (0-48 h) and concentration- (0-35 μM) dependent manner (Fig. 2D). An intracellular calcium chelator, BAPTA-AM (500 nM), was used to pre-treat U87 cells, and the ROS production induced by SKF83959 was decreased, indicating that inhibition of intracellular Ca^{2+} level prevented the aberrantly over-increased oxidative stress (Fig. 2E).

DRD1-agonist-induced-GBM cell apoptosis is related to ER stress and mitochondrial dysfunction. To investigate the mechanism involved in DRD1-agonist-induced apoptosis of U87 cells, the downstream molecules of increased intracellular Ca^{2+} level and ROS generation were investigated. Excessive oxidative stress has been implicated in activation of ER stress and destruction of mitochondrial outer membrane, triggering apoptosis (28,34). Therefore, to reveal the effect of SKF83959 treatment on mitochondria, the mitochondrial

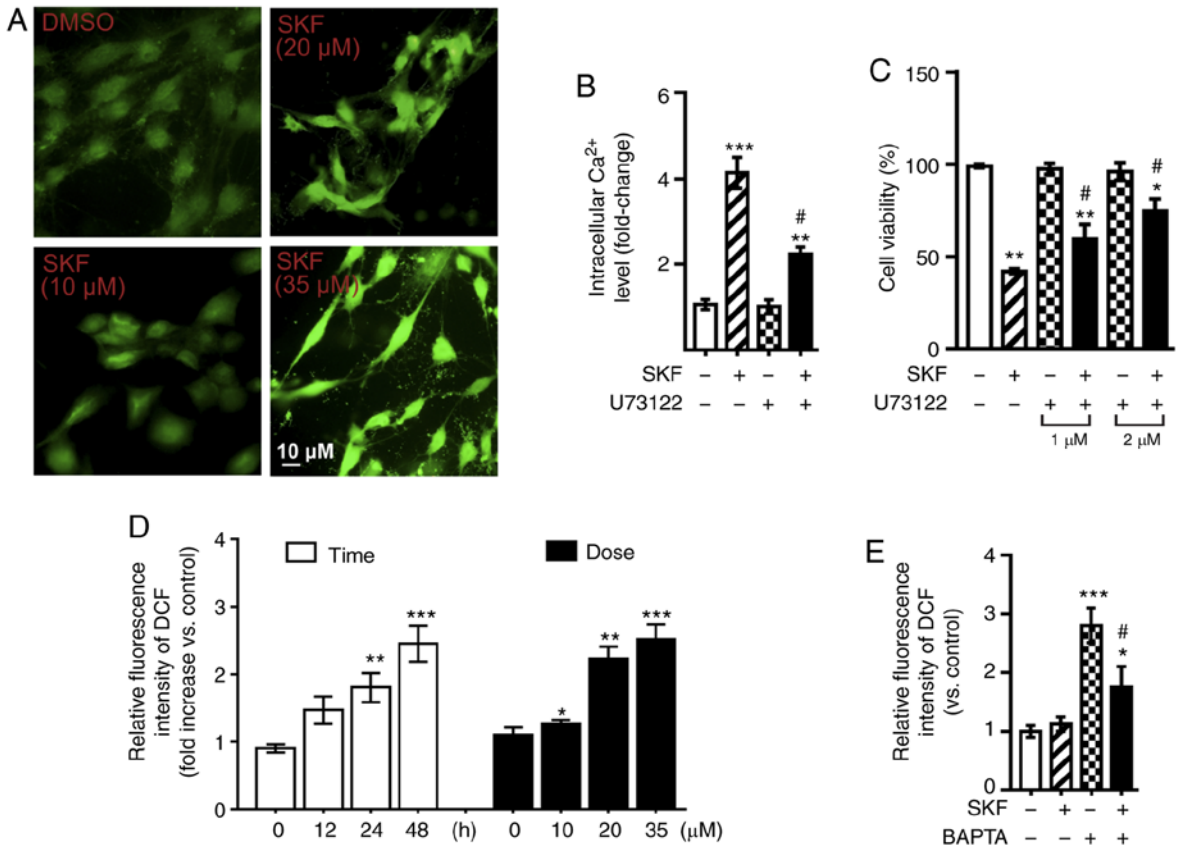

Figure 2. DRD1 agonist increases PLC-dependent intracytosolic Ca^{2+} levels and induces oxidative stress. (A) Fluorescence microscopy was used to measure intracellular Ca^{2+} in Fluo-4 AM-loaded U87 cells treated with various doses of SKF83959 (0, 10, 20, and 35 μM) for 30 min. Scale bar, 10 μm. (B) Intracellular Ca^{2+} measurements in Fluo-4-AM-loaded U87 cells treated with SKF83959 (35 μM) and/or U73122 (2 μM,) for 60 min. (C) Viability of U87 cells treated with SKF83959 and/or U73122 (1-2 μM) for 48 h. (D) Relative fluorescence intensity of DCF (representing ROS levels) was analysed in U87 cells treated with SKF83959 at 0-35 μM or for 0-48 h. (E) Relative fluorescence intensity of DCF (representing ROS level) was analysed in U87 cells treated with SKF83959 and/or BAPTA (500 nM) for 48 h. *P<0.05, **P<0.01, and ***P<0.001 (vs. Ctrl); $^{\#}$P<0.05 (vs. U87 cells treated with SKF83959). DRD1, dopamine receptor D1; PLC, phospholipase C; ROS, reactive oxygen species; Ctrl, control; SKF, SKF83959.

membrane potential-dependent staining assay (Mito-Tracker Red CMXRos kit) was firstly employed to evaluate the mitochondrial transmembrane potential in U87 cells. The red fluorescence intensity was significantly decreased by SKF83959 treatment (35 μM), suggesting probable mitochondrial injury. However, co-treatment with BAPTA-AM (500 nM) partially reversed the fluorescence intensity in U87 cells compared with SKF83959 treatment alone, suggesting the aforementioned signalling changes were dependent on the increase in intracellular Ca^{2+} level (Fig. 3A). Then, COX IV, which was attached to the surface of the mitochondrial membrane and Bcl-2, which suppressed activation of caspases by inhibiting the release of Cyt *c* into the cytoplasm, were assessed (28). The protein level of COX IV was markedly increased while the protein level of Bcl-2 was significantly decreased in U87 cells under SKF83959 treatment (Fig. 3B). Furthermore, the protein levels of Cyt *c* in U87 cells under different doses of SKF83959 treatment (0, 10, 20, 35 μM) were measured after the mitochondrial and cytosolic fraction. The mitochondrial Cyt *c* was decreased while the cytosolic Cyt *c* was significantly increased, which suggested damage in the mitochondrial membrane in response to activation of mitochondrial apoptosis (Fig. 3C). Western blotting was also used to assess the ER stress markers BiP (GRP78) and CHOP, and the results revealed significant increases in their protein levels in SKF83959-treated U87 cells in a time-dependent (0-48 h) and concentration-dependent (0-35 μM) manner (Fig. 3D) (42,43).

DRD1 agonist-activated calpain signalling, induces ER stress and mitochondrial dysfunction and eventual apoptosis. Activation of PLC leads to Ca^{2+} release from intracellular Ca^{2+} stores including ER, and increased intracytosolic Ca^{2+} concentration activates calpains (9,39). Calpain 1 (μ-calpain) and calpain 2 (m-calpain) both contain a small regulatory 30-kDa subunit, which is activated by increased intracellular Ca^{2+} (9,44). Increased calpain levels were determined by western blotting in U87 cells treated with SKF83959 in a time-dependent (0-48 h) and concentration-dependent (0-35 μM) manner (Fig. 4A). Calpain inhibitor calpastatin was applied to reduce calpain activation. Western blotting verified the inhibitory effect of calpastatin on calpains by decreasing protein levels of the small regulatory subunit of calpains in the absence and presence of SKF83959 treatment (Fig. 4B). CCK-8 assays revealed that co-treatment with calpastatin decreased the cytotoxic effect of DRD1 agonist on U87 cells in a concentration-dependent manner (25 nM-1 μM) (Fig. 4C). The microscopic *in vitro* images displayed the reversed inhibitory effect of SKF83959, (35 μM, incubation for 48 h) when cotreated with calpastatin (500 nM,

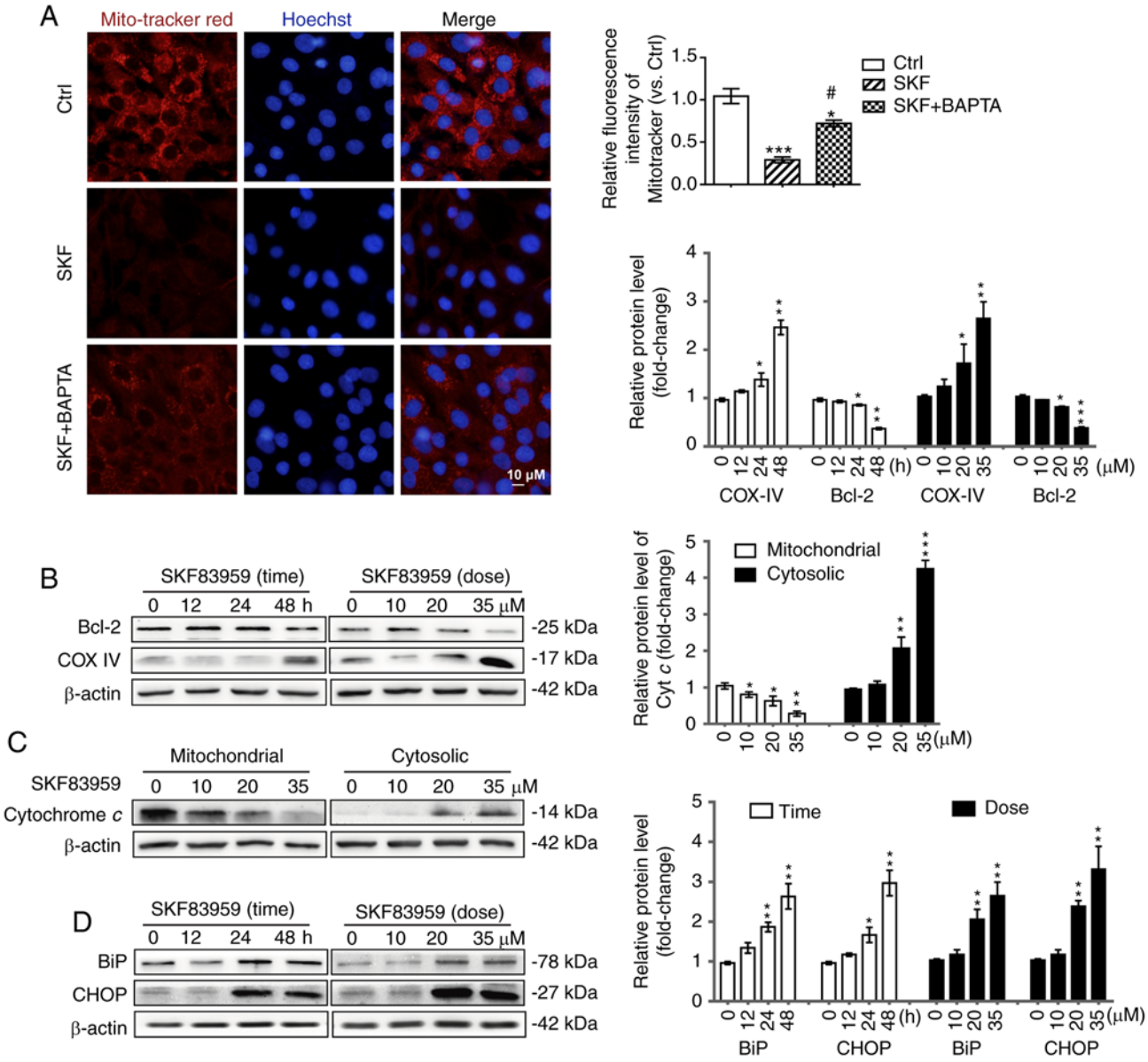

Figure 3. DRD1-agonist-induced-GBM cell apoptosis is related to ER stress and mitochondrial dysfunction. (A) Mitochondrial membrane potential was detected using Mito-tracker Red. Fluorescence microscopy was used to measure fluorescence intensity in U87 cells treated with SKF83959 (35 μM) and/or BAPTA (500 nM) for 24 h. Scale bars, 10 μm. (B) The protein levels of COX IV and Bcl-2 in U87 cells treated with SKF83959 at 0-35 μM or for 0-48 h were determined by western blotting. Quantification of relative protein levels is presented on the right (n=3). (C) Mitochondrial and cytosolic protein levels of Cyt *c* in U87 cells treated with various doses of SKF83959 (0, 10, 20, 35 μM) for 48 h were measured by western blotting. (D) Expression of BiP, CHOP, and β-actin in U87 cells treated with SKF83959 at 0-35 μM or for 0-48 h was determined by western blotting. Quantification of relative protein levels is presented on the right (n=3). *P<0.05, **P<0.01, and ***P<0.001 (vs. Ctrl); $^{\#}$P<0.05 (vs. U87 cells treated with SKF83959). DRD1, dopamine receptor D1; GBM, glioblastoma; ER, endoplasmic reticulum; Cyt *c*, cytochrome *c*; Ctrl, control; SKF, SKF83959.

incubation for 48 h), on U87 cells (Fig. 4D). The aforementioned observations suggest the important role of calpains in the SKF83959 treatment-induced GBM cell apoptosis. To determine whether calpains were also involved in the ER stress and mitochondrial dysfunction leading to apoptotic cascade, the respective markers including cleaved caspase-3 and BiP were assessed by western blotting. Compared with SKF83959 treatment alone, co-treatment with the calpain inhibitor, calpastatin, significantly decreased the expression levels of cleaved caspase-3 and BiP, which suggested that the over-activated calpain signalling contributed to mitochondrial dysfunction and ER stress in U87 cells, followed by apoptosis during SKF83959 treatment (Fig. 4E).

DRD1-agonist-induced-calpain activation, followed by GBM growth inhibition, is observed in vivo. The *in vivo* inhibitory efficacy of SKF83959 was verified by observing a 36.3% reduction of tumour size in GBM xenograft models (U87 cells injected into the flanks of immunocompromised BALB/c nude mice) receiving SKF83959 treatment (1 mg/kg/day) compared with the control group (mice treated with the same amount of saline, n=5 in each group) (Fig. 5A). In order to investigate the *in vivo* molecular pathway involving calpain activation, ER stress and mitochondrial dysfunction, western blot analysis of calpains, BiP and Cyt *c* was performed in tumours treated with SKF83959 or control saline. It was revealed that increases in protein levels of calpains, BiP and Cyt *c* in SKF83959-treated

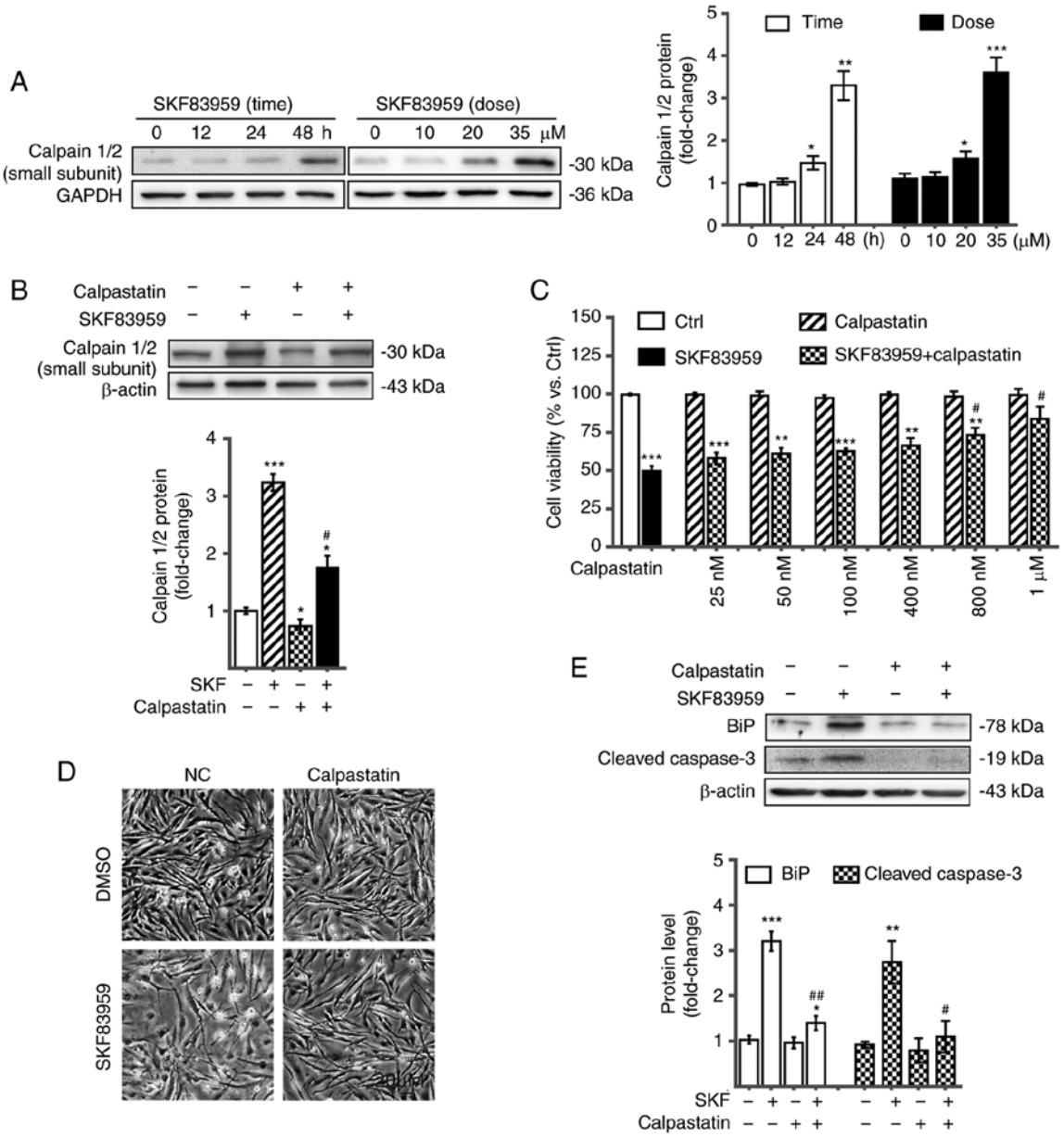

Figure 4. DRD1 agonist-activated calpain signalling, induces ER stress and mitochondrial dysfunction, which leads to apoptosis. (A) Expression of the small subunit of calpains in U87 cells treated with SKF83959 at 0-35 μM or for 0-48 h was determined by western blotting. Quantification of the relative protein levels is presented on the right (n=3). (B) Expression of the small subunit of calpains in U87 cells treated with SKF83959 in the presence or absence of calpastatin, a calpain inhibitor, was determined by western blotting. (C) Viability of U87 cells with SKF83959 co-treated with the calpain inhibitor calpastatin at 25 nM-1 μM for 48 h. (D) Microscopic images of U87 cells treated with calpastatin (500 nM) and/or SKF83959 (35 μM) for 48 h. Scale bars, 20 μm. (E) Expression of BIP and cleaved caspase-3 in U87 cells treated with SKF83959 in the presence or absence of calpastatin. *P<0.05, **P<0.01, and ***P<0.001 (vs. Ctrl); $^{\#}$P<0.05 and $^{\#\#}$P<0.01 (vs. U87 cells treated with SKF83959). DRD1, dopamine receptor D1; ER, endoplasmic reticulum; Ctrl, control; SKF, SKF83959.

GBM tumours were consistent with the *in vitro* observations in U87 cells (Fig. 5B). In addition, immunohistochemical (IHC) staining of calpains on xenograft GBM sections was performed, and it was revealed that calpains exhibited higher expression in tumours treated with SKF83959 compared with controls (percentage of calpain-positive cells of the SKF83959 group was 39.1 vs. 12.6% in the control group), which provided *in vivo* evidence for the upregulation of calpains under SKF83959 treatment (Fig. 5C). Considering that DRD1 agonist induced GBM cell apoptosis by dysregulated calpain activation, IHC staining of calpains was performed on human GBM tissues, and evidence of increased calpain expression compared with control brain tissues, was determined (Fig. 5D). These data indicated that calpains may be involved in GBM progression, and that therapeutic approaches regarding calpain expression and activity regulation may be a potential avenue for GBM treatment.

Discussion

Management of glioblastoma remains challenging; thus, it is mandatory to investigate novel treatments for improved patient outcome. Growing evidence implicates the role of dopaminergic signalling in pathogenesis of GBM, and in dopamine-receptor-regulator-mediated chemotherapy involving apoptosis of GBM (45,46). Calpains are also implicated in

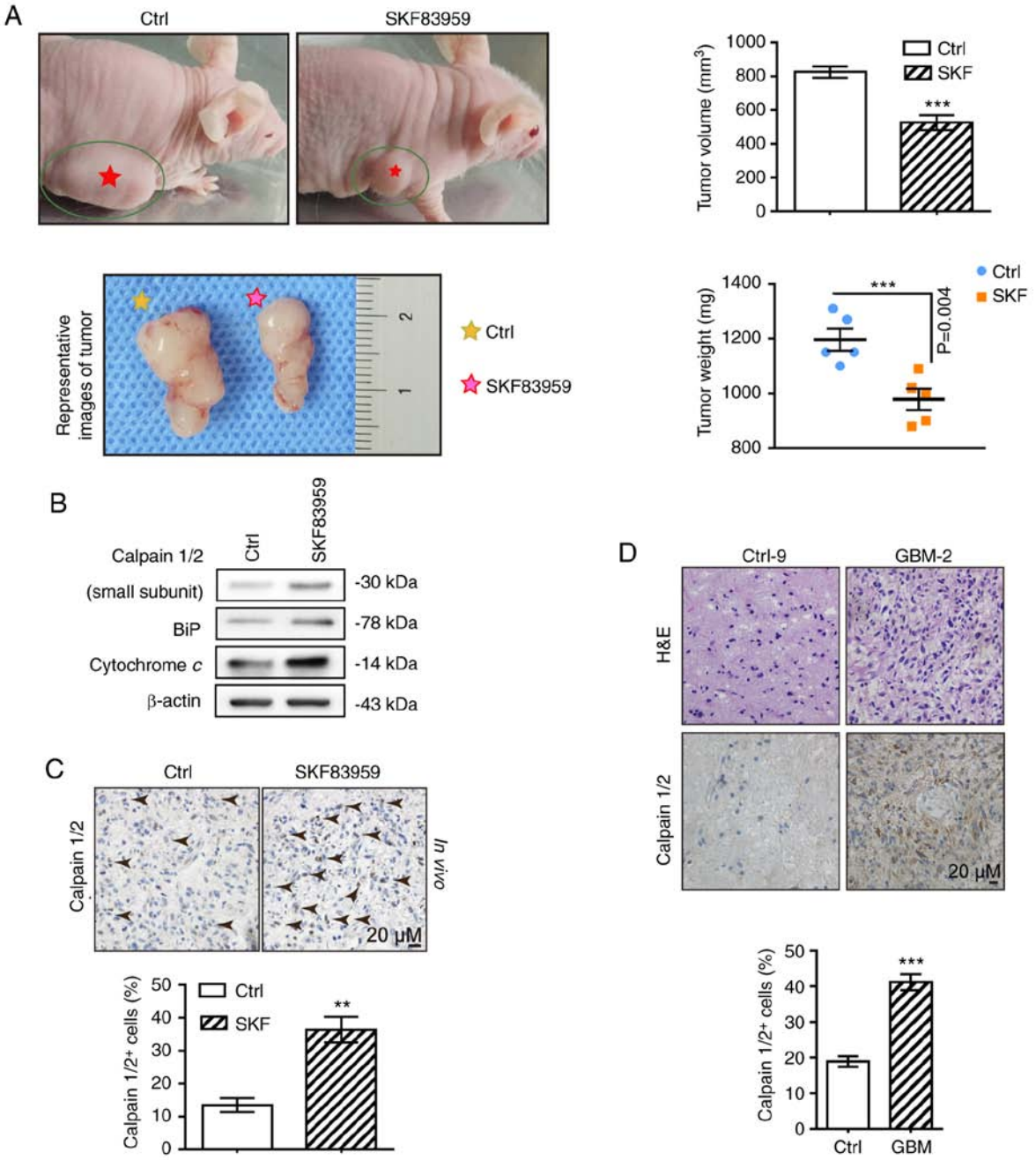

Figure 5. DRD1-agonist-induced-calpain activation, ER stress and mitochondrial dysfunction are observed *in vivo*. (A) Representative GBM xenograft mice bearing subcutaneously implanted tumours as well as images of tumours that had received SKF83959 treatment or control saline are presented at the endpoint (images on the left). Statistical analysis of tumour volume and weight under different treatment conditions was performed (images on the right). (B) Expression of calpain1/2, BiP and Cyt *c* in tumours measured across two groups by western blotting. (C) IHC staining for calpains in xenograft tumours treated with SKF83959 or saline. Scale bars, 20 μm. (D) IHC staining for calpain1/2 in GBM and control brain tissues. H&E-stained GBM sections revealing necrosis, dense cellularity and perinecrotic pseudo-palisading cells. Scale bars, 20 μM. **P<0.01, and ***P<0.001 (vs. Ctrl). DRD1, dopamine receptor D1; ER, endoplasmic reticulum; GBM, glioblastoma; Ctrl, control; SKF, SKF83959.

tumour migration and invasion of GBM (9,47). It is documented that through activation of ER stress, oxidative stress, and mitochondrial injury, calpains trigger apoptosis (29,33,34). However, the role of calpains in dopamine-receptor-regulator-mediated apoptosis in GBM was not fully elucidated. In the present study, the DRD1 agonist, SKF83959, was applied to GBM cells and ER stress and mitochondrial injury-dependent GBM cell apoptosis were observed. The mechanistic study revealed that the well expressed intracytosolic Ca^{2+}-activated calpains in GBM cells were the key signalling factors during the apoptotic cascade. Application of calpain inhibitor calpastatin significantly reversed the increase in mitochondrial injury and ER stress markers and eventually ameliorated the GBM cell apoptosis during SKF83959 treatment.

Previous studies have described that DRs can bind to Gq protein, stimulate PLC and result in hydrolysis of phosphoinositide (48,49). SKF83959, a selective DRD1 agonist, activates the PLC/IP3 pathway, which is followed by an increase in cytosolic Ca^{2+} (50-52). The present data validated the signalling pathway and it was observed that

SKF83959-stimulated increases in Ca^{2+} levels, and even apoptosis, were abolished by the PLC inhibitor, U73122, in U87 cells, which was a novel finding regarding intracellular Ca^{2+} release via PLC activation in human GBM cell lines. The increased intracellular Ca^{2+} levels upregulated calpains, which are intracellular cysteine proteases (9,39). The present data suggested that increased Ca^{2+} levels following PLC activation could enhance calpain activity after SKF83959 treatment. The calcium chelator, BAPTA-AM, reversed the increased calpain levels, calpain-mediated mitochondrial injury, and ER stress, suggesting a pivotal role of intracellular Ca^{2+} between DRD1 agonist and calpain-induced GBM apoptosis.

Calpains are multi-subunit, Ca^{2+}-activated proteases and are necessary for various cellular functions such as genetic regulation, cytoskeletal remodelling and cell mobility. However, there are still many counterviews regarding the role of calpains in GBM cell migration and survival (12,16,17,53). For instance, calpain inhibitors were revealed to have a protective effect on neurons under ischemic or cytotoxic conditions (54,55). In the GBM cell line, C6, the cytotoxic effect of *Crocus sativus* L. was significantly reversed by MDL-28170 (a calpain inhibitor), implicating calpains as possible cell death mediators (54). However, Jang *et al* reported a positive effect of calpain 2 on GBM invasion by identifying the complex signalling transduction of tumour cells in the brain environment (14). Calpains have also been revealed to activate matrix metalloproteinase secretion and enhance invasive potential through transformation of growth factor-β-inducible gene-h3 and integrin α5β1 in U87 cells (17). Another *in vivo* study revealed, by conducting a xenograft GBM model in zebrafish brain, that calpains are also necessary for the dispersal and migration of GBM cells along the blood vessels (16).

The pivotal factor defining the effects of calpains is the impact of Ca^{2+} elevation on their activation, and the uncontrolled elevation of Ca^{2+} level may lead to prolonged and dysregulated calpain activation, followed by cellular damage (9,56). Previous studies have reported that under pathological conditions, the dysregulation of calpain activity could cause uncontrolled protein cleavage, resulting in irreversible cellular injury. For instance, under environmental stress stimuli, the hydrolysis of Beclin-1 mediated by calpains was revealed in nerve tissues (56-59). The present data support the hypothesis that activation of calpains by high levels of intracellular Ca^{2+} and oxidative stress negatively affect cell fate and survival of GBM, suggesting a potential therapeutic target for human GBM treatment regarding calpain expression and activity regulation.

Mechanistic studies concerning the signalling transduction between calpains and apoptosis through oxidative stress, induction of mitochondrial injury, and activation of ER stress have recently been reported (60-62). Fluoride-induced bone damage has been revealed to be related to apoptosis induced by calpain-dependent ER stress and mitochondrial dysfunction (60). Lv *et al* demonstrated that taurine attenuated hypoxia-induced cardiomyocyte damage by supressing calpain-mediated, mitochondria-related apoptosis (61). Activation of ER stress and calpains was detected during hyperuricemia-triggered cellular apoptosis *in vivo*, which could be alleviated by calpain inhibitors or knockdown of calpain 1 expression (62). In human retinal epithelial cells, the decreased expression of calpain 2 has also been reported to inhibit starvation-triggered apoptosis (63). The present data were consistent with the aforementioned evidence that calpain activation induced by a DRD1 agonist could trigger an apoptotic cascade through damage to mitochondrial function and exacerbation of ER stress.

In summary, GBM cell apoptosis in human GBM U87 cells under treatment with DRD1 agonist SKF83959 was demonstrated. SKF83959 administration increased the intracellular Ca^{2+} level through PLC signalling, and the downstream calpains were activated and dysregulated accordingly, which led to mitochondrial injury and ER stress, followed by apoptosis. These findings suggested the potential therapeutic effect of DRD1 agonist against GBM and may require further investigations for human GBM treatment regarding calpain expression and activity regulation.

Acknowledgements

Not applicable.

Funding

The present research was funded by the National Natural Science Foundation of China (NSFC) (grant nos. 81430021 and 81771521).

Availability of data and materials

All data generated or analysed during this study are included in this published article.

Authors' contributions

KY and WL designed the study. KY and RX collected human GBM samples and provided the nude mice. KY performed experiments (cell culture analysis, immunohistochemistry, flow cytometric analysis, cell cycle, and xenograft experiments) and analysed the data. KY wrote and edited the manuscript. RX and WL edited and reviewed the manuscript for important intellectual content. All authors have read and approved the final manuscript.

Ethics approval and consent to participate

The study was approved by the Ethics Committee of the Second Hospital of Dalian Medical University (DMU) (Dalian, China) (approval no. 2018052) and followed the ethical guidelines of the Declaration of Helsinki. Written informed consent was obtained from all patients whose tissues were used in this study. Mice were purchased from the Institute of Genome-Engineered Animal Models of DMU and were kept under specific pathogen-free conditions. The study protocol was approved by the Animal Ethics Committee of DMU (approval no. 2018112).

Patient consent for publication

Not applicable.

Competing interests

The authors declare that they have no competing interests.

References

1. Omuro A and DeAngelis LM: Glioblastoma and other malignant gliomas: A clinical review. JAMA 310: 1842-1850, 2013.
2. Ostrom QT, Gittleman H, Xu J, Kromer C, Wolinsky Y, Kruchko C and Barnholtz-Sloan JS: CBTRUS statistical report: Primary brain and other central nervous system tumors diagnosed in the united states in 2009-2013. Neuro Oncol 18 (Suppl 5): v1-v75, 2016.
3. Tabatabai G and Wakimoto H: Glioblastoma: State of the art and future perspectives. Cancers (Basel) 11: 1091, 2019.
4. Claes A, Idema AJ and Wesseling P: Diffuse glioma growth: A guerilla war. Acta Neuropathol 114: 443-458, 2007.
5. de Groot JF, Fuller G, Kumar AJ, Piao Y, Eterovic K, Ji Y and Conrad CA: Tumor invasion after treatment of glioblastoma with bevacizumab: Radiographic and pathologic correlation in humans and mice. Neuro Oncol 12: 233-242, 2010.
6. Lee DH, Ryu HW, Won HR and Kwon SH: Advances in epigenetic glioblastoma therapy. Oncotarget 8: 18577-18589, 2017.
7. Clapham DE: Calcium signaling. Cell 131: 1047-1058, 2007.
8. Kim KW, Choi CH, Kim TH, Kwon CH, Woo JS and Kim YK: Silibinin inhibits glioma cell proliferation via Ca2+/ROS/MAPK-dependent mechanism in vitro and glioma tumor growth in vivo. Neurochem Res 34: 1479-1490, 2009.
9. Goll DE, Thompson VF, Li H, Wei W and Cong J: The calpain system. Physiol Rev 83: 731-801, 2003.
10. Carragher NO and Frame MC: Calpain: A role in cell transformation and migration. Int J Biochem Cell Biol 34: 1539-1543, 2002.
11. Roumes H, Leloup L, Dargelos E, Brustis JJ, Daury L and Cottin P: Calpains: Markers of tumor aggressiveness? Exp Cell Res 316: 1587-1599, 2010.
12. Cortesio CL, Chan KT, Perrin BJ, Burton NO, Zhang S, Zhang ZY and Huttenlocher A: Calpain 2 and PTP1B function in a novel pathway with Src to regulate invadopodia dynamics and breast cancer cell invasion. J Cell Biol 180: 957-971, 2008.
13. Mamoune A, Luo JH, Lauffenburger DA and Wells A: Calpain-2 as a target for limiting prostate cancer invasion. Cancer Res 63: 4632-4640, 2003.
14. Jang HS, Lal S and Greenwood JA: Calpain 2 is required for glioblastoma cell invasion: Regulation of matrix metalloproteinase 2. Neurochem Res 35: 1796-1804, 2010.
15. Vo TM, Burchett R, Brun M, Monckton EA, Poon HY and Godbout R: Effects of nuclear factor I phosphorylation on calpastatin (CAST) gene variant expression and subcellular distribution in malignant glioma cells. J Biol Chem 294: 1173-1188, 2019.
16. Lal S, La Du J, Tanguay RL and Greenwood JA: Calpain 2 is required for the invasion of glioblastoma cells in the zebrafish brain microenvironment. J Neurosci Res 90: 769-781, 2012.
17. Ma J, Cui W, He SM, Duan YH, Heng LJ, Wang L and Gao GD: Human U87 astrocytoma cell invasion induced by interaction of βig-h3 with integrin α5β1 involves calpain-2. PLoS One 7: e37297, 2012.
18. Su Y, Cui Z, Li Z and Block ER: Calpain-2 regulation of VEGF-mediated angiogenesis. FASEB J 20: 1443-1451, 2006.
19. Kritis A, Pourzitaki C, Klagas I, Chourdakis M and Albani M: Proteases inhibition assessment on PC12 and NGF treated cells after oxygen and glucose deprivation reveals a distinct role for aspartyl proteases. PLoS One 6: e25950, 2011.
20. Samarghandian S, Tavakkol Afshari J and Davoodi S: Suppression of pulmonary tumor promotion and induction of apoptosis by *Crocus sativus* L. extraction. Appl Biochem Biotechnol 164: 238-247, 2011.
21. Scaffidi C, Kischkel FC, Krammer PH and Peter ME: Analysis of the CD95 (APO-1/Fas) death-inducing signaling complex by high-resolution two-dimensional gel electrophoresis. Methods Enzymol 322: 363-373, 2000.
22. Wick W, Wild-Bode C, Frank B and Weller M: BCL-2-induced glioma cell invasiveness depends on furin-like proteases. J Neurochem 91: 1275-1283, 2004.
23. Stegh AH, Kim H, Bachoo RM, Forloney KL, Zhang J, Schulze H, Park K, Hannon GJ, Yuan J, Louis DN, *et al*: Bcl2L12 inhibits post-mitochondrial apoptosis signaling in glioblastoma. Genes Dev 21: 98-111, 2007.
24. Sastry PS and Rao KS: Apoptosis and the nervous system. J Neurochem 74: 1-20, 2000.
25. Zimmermann KC, Bonzon C and Green DR: The machinery of programmed cell death. Pharmacol Ther 92: 57-70, 2001.
26. Ashe PC and Berry MD: Apoptotic signaling cascades. Prog Neuropsychopharmacol Biol Psychiatry 27: 199-214, 2003.
27. Rao RV, Ellerby HM and Bredesen DE: Coupling endoplasmic reticulum stress to the cell death program. Cell Death Differ 11: 372-380, 2004.
28. Charlier E, Relic B, Deroyer C, Malaise O, Neuville S, Collée J, Malaise MG and De Seny D: Insights on molecular mechanisms of chondrocytes death in osteoarthritis. Int J Mol Sci 17: 2146, 2016.
29. Lepetsos P and Papavassiliou AG: ROS/oxidative stress signaling in osteoarthritis. Biochim Biophys Acta 1862: 576-591, 2016.
30. Shiraishi H, Okamoto H, Yoshimura A and Yoshida H: ER stress-induced apoptosis and caspase-12 activation occurs downstream of mitochondrial apoptosis involving Apaf-1. J Cell Sci 119: 3958-3966, 2006.
31. Li D, Xie G and Wang W: Reactive oxygen species: The 2-edged sword of osteoarthritis. Am J Med Sci 344: 486-490, 2012.
32. Bolisetty S and Jaimes EA: Mitochondria and reactive oxygen species: Physiology and pathophysiology. Int J Mol Sci 14: 6306-6344, 2013.
33. Wu L, Liu H, Li L, Liu H, Cheng Q, Li H and Huang H: Mitochondrial pathology in osteoarthritic chondrocytes. Curr Drug Targets 15: 710-719, 2014.
34. Ye W, Zhu S, Liao C, Xiao J, Wu Q, Lin Z and Chen J: Advanced oxidation protein products induce apoptosis of human chondrocyte through reactive oxygen species-mediated mitochondrial dysfunction and endoplasmic reticulum stress pathways. Fundam Clin Pharmacol 31: 64-74, 2017.
35. Guan L, Che Z, Meng X, Yu Y, Li M, Yu Z, Shi H, Yang D and Yu M: MCU Up-regulation contributes to myocardial ischemia-reperfusion Injury through calpain/OPA-1-mediated mitochondrial fusion/mitophagy Inhibition. J Cell Mol Med 23: 7830-7843, 2019.
36. Cho SO, Lim JW and Kim H: Oxidative stress induces apoptosis via calpain- and caspase-3-mediated cleavage of ATM in pancreatic acinar cells. Free Radic Res: Aug 30, 2019 (Epub ahead of print). doi: 10.1080/10715762.2019.1655145.
37. Yang K, Wei M, Yang Z, Fu Z, Xu R, Cheng C, Chen X, Chen S, Dammer E and Le W: Activation of dopamine receptor D1 inhibits glioblastoma tumorigenicity by regulating autophagic activity. Cell Oncol (Dordr) 43: 1175-1190, 2020.
38. Jin LQ, Goswami S, Cai G, Zhen X and Friedman E: SKF83959 selectively regulates phosphatidylinositol-linked D1 dopamine receptors in rat brain. J Neurochem 85: 378-386, 2003.
39. Liu J, Wang F, Huang C, Long LH, Wu WN, Cai F, Wang JH, Ma LQ and Chen JG: Activation of phosphatidylinositol-linked novel D1 dopamine receptor contributes to the calcium mobilization in cultured rat prefrontal cortical astrocytes. Cell Mol Neurobiol 29: 317-328, 2009.
40. Panchalingam S and Undie AS: SKF83959 exhibits biochemical agonism by stimulating [(35)S]GTP gamma S binding and phosphoinositide hydrolysis in rat and monkey brain. Neuropharmacology 40: 826-837, 2001.
41. Tran TD, Gimble JM and Cheng H: Vasopressin-induced Ca(2+) signals in human adipose-derived stem cells. Cell Calcium 59: 135-139, 2016.
42. Malhotra JD and Kaufman RJ: Endoplasmic reticulum stress and oxidative stress: A vicious cycle or a double-edged sword? Antioxid Redox Signal 9: 2277-2293, 2007.
43. Uehara Y, Hirose J, Yamabe S, Okamoto N, Okada T, Oyadomari S and Mizuta H: Endoplasmic reticulum stress-induced apoptosis contributes to articular cartilage degeneration via C/EBP homologous protein. Osteoarthritis Cartilage 22: 1007-1017, 2014.
44. Williams A, Sarkar S, Cuddon P, Ttofi EK, Saiki S, Siddiqi FH, Jahreiss L, Fleming A, Pask D, Goldsmith P, *et al*: Novel targets for Huntington's disease in an mTOR-independent autophagy pathway. Nat Chem Biol 4: 295-305, 2008.
45. Moreno-Smith M, Lu C, Shahzad MM, Pena GN, Allen JK, Stone RL, Mangala LS, Han HD, Kim HS, Farley D, *et al*: Dopamine blocks stress-mediated ovarian carcinoma growth. Clin Cancer Res 17: 3649-3659, 2011.
46. Lan YL, Wang X, Xing JS, Yu ZL, Lou JC, Ma XC and Zhang B: Anti-cancer effects of dopamine in human glioma: Involvement of mitochondrial apoptotic and anti-inflammatory pathways. Oncotarget 8: 88488-88500, 2017.
47. Franco SJ and Huttenlocher A: Regulating cell migration: Calpains make the cut. J Cell Sci 118: 3829-3838, 2005.
48. Friedman E, Jin LQ, Cai GP, Hollon TR, Drago J, Sibley DR and Wang HY: D1-like dopaminergic activation of phosphoinositide hydrolysis is independent of D1A dopamine receptors: Evidence from D1A knockout mice. Mol Pharmacol 51: 6-11, 1997.

49. Panchalingam S and Undie AS: Physicochemical modulation of agonist-induced [35s]GTPgammaS binding: Implications for coexistence of multiple functional conformations of dopamine D1-like receptors. J Recept Signal Transduct Res 25: 125-146, 2005.
50. Zhen X, Goswami S and Friedman E: The role of the phosphatidyinositol-linked D1 dopamine receptor in the pharmacology of SKF83959. Pharmacol Biochem Behav 80: 597-601, 2005.
51. Ming Y, Zhang H, Long L, Wang F, Chen J and Zhen X: Modulation of Ca2+ signals by phosphatidylinositol-linked novel D1 dopamine receptor in hippocampal neurons. J Neurochem 98: 1316-1323, 2006.
52. Rashid AJ, So CH, Kong MM, Furtak T, El-Ghundi M, Cheng R, O'Dowd BF and George SR: D1-D2 dopamine receptor heterooligomers with unique pharmacology are coupled to rapid activation of Gq/11 in the striatum. Proc Natl Acad Sci USA 104: 654-659, 2007.
53. Yousefi S, Perozzo R, Schmid I, Ziemiecki A, Schaffner T, Scapozza L, Brunner T and Simon HU: Calpain-mediated cleavage of Atg5 switches autophagy to apoptosis. Nat Cell Biol 8: 1124-1132, 2006.
54. Giakoumettis D, Pourzitaki C, Vavilis T, Tsingotjidou A, Kyriakoudi A, Tsimidou M, Boziki M, Sioga A, Foroglou N and Kritis A: *Crocus sativus* L. causes a non apoptotic calpain dependent death in C6 rat glioma cells, exhibiting a synergistic effect with temozolomide. Nutr Cancer 71: 491-507, 2019.
55. Schumacher PA, Siman RG and Fehlings MG: Pretreatment with calpain inhibitor CEP-4143 inhibits calpain I activation and cytoskeletal degradation, improves neurological function, and enhances axonal survival after traumatic spinal cord injury. J Neurochem 74: 1646-1655, 2000.
56. Kim JS, Wang JH, Biel TG, Kim DS, Flores-Toro JA, Vijayvargiya R, Zendejas I and Behrns KE: Carbamazepine suppresses calpain-mediated autophagy impairment after ischemia/reperfusion in mouse livers. Toxicol Appl Pharmacol 273: 600-610, 2013.
57. Kim JS, Nitta T, Mohuczy D, O'Malley KA, Moldawer LL, Dunn WA Jr and Behrns KE: Impaired autophagy: A mechanism of mitochondrial dysfunction in anoxic rat hepatocytes. Hepatology 47: 1725-1736, 2008.
58. Russo R, Berliocchi L, Adornetto A, Varano GP, Cavaliere F, Nucci C, Rotiroti D, Morrone LA, Bagetta G and Corasaniti MT: Calpain-mediated cleavage of Beclin-1 and autophagy deregulation following retinal ischemic injury in vivo. Cell Death Dis 2: e144, 2011.
59. Song F, Han X, Zeng T, Zhang C, Zou C and Xie K: Changes in beclin-1 and micro-calpain expression in tri-ortho-cresyl phosphate-induced delayed neuropathy. Toxicol Lett 210: 276-284, 2012.
60. Wang J, Yang J, Cheng X, Xiao R, Zhao Y, Xu H, Zhu Y, Yan Z, Ommati MM, Manthari RK and Wang J: Calcium alleviates fluoride-induced bone damage by inhibiting endoplasmic reticulum stress and mitochondrial dysfunction. J Agric Food Chem 67: 10832-10843, 2019.
61. Lv Q, Yang J, Wang Y, Liu M, Feng Y, Wu G, Lin S, Yang Q and Hu J: Taurine prevented hypoxia induced chicken cardiomyocyte apoptosis through the inhibition of mitochondrial pathway activated by Calpain-1. Adv Exp Med Biol 1155: 451-462, 2019.
62. Yan M, Chen K, He L, Li S, Huang D and Li J: Uric acid induces cardiomyocyte apoptosis via activation of Calpain-1 and endoplasmic reticulum stress. Cell Physiol Biochem 45: 2122-2135, 2018.
63. Zhang Y, Ren S, Liu Y, Gao K, Liu Z and Zhang Z: Inhibition of starvation-triggered endoplasmic reticulum stress, autophagy, and apoptosis in ARPE-19 cells by taurine through modulating the expression of Calpain-1 and Calpain-2. Int J Mol Sci 18: 2146, 2017.